International Journal of Technology (2018) 5: 866-875
ISSN 2086-9614

A COMPACT MICROSTRIP SLOTTED ANTENNA FOR DUAL-BAND RFID APPLICATIONS

Ahmed Elhamraoui[1*], Elhassane Abdelmounim[1], Jamal Zbitou[2], Hamid Bennis[3], Mohamed Latrach[4], Abdelaali Tajmouati[2]

[1]*ASTI Laboratory, FSTS, Hassan 1st University, Settat-Morocco*
[2]*MEET Laboratory, FSTS, Hassan 1st University, Settat, Morocco*
[3]*TIM Research Team, EST of Meknes, Moulay Ismail University, Meknes, Morocco*
[4]*Microwave Group, ESEO, Angers, France*

(Received: October 2017 / Revised: July 2018 / Accepted: September 2018)

ABSTRACT

This paper presents a new dual-band microstrip antenna with embedded slots on a rectangular radiator. It is capable of operating in the two radio frequency identification (RFID) frequency bands simultaneously (UHF and microwave) and has a miniaturized size designed to be easily integrated into portable RFID readers. The simulation results, carried out using the two commercial software packages CST Microwave Studio electromagnetic and ADS, show stable radiation pattern performances and good matching input impedance at the desired operating frequencies. The proposed antenna has overall dimensions of 47×46 mm^2 and is mounted on an FR4 substrate with dielectric permittivity constant 4.4, thickness 1.6 mm and loss tangent 0.025. The creation of a prototype of the proposed optimal antenna allowed validation of the dual operating bands with -10 dB return-loss bandwidths of approx. 28 MHz centred at 0.868 GHz and of approx. 90 MHz centred at 2.45 GHz, which shows that the proposed antenna is a good candidate for implementation in handheld RFID readers.

Keywords: Antenna; Dual-frequency operation; L-shaped slot; Microstrip fed; RFID (Radio Frequency Identification); Slot antenna

1. INTRODUCTION

During the last few years, radio frequency identification (RFID) applications have been growing significantly in many fields, such as medicine, supply chain, intelligent trace, shop security and particularly in the area of electronic article surveillance, in which it has become one of the most important techniques (Brown, 2007; Finkenzeller, 2010; Poespawati & Nugroho, 2016). The RFID system generally consists of two elements: the tag and the reader. The RFID reader acts as an interrogator equipped with an antenna that sends a radio frequency interrogation signal and receives the backscattered signal containing the data stored in the tag, which is composed of an integrated circuit chip connected to an antenna. The basic block diagram of an RFID system is illustrated in Figure 1.

The RFID system can be described as a fusion of different modern technologies from several areas: monolithic integrated circuits; identification technology; coding and modulation (Mujahid & Najam-ul-islam, 2017); cryptography, providing the secure mutual authentication between reader and tag (Paret, 2008; El Hamraoui et al., 2016); and wireless transmission.

* Corresponding author's email: a.elhamraoui@outlook.fr, Tel. +212-523400736, Fax. +212-523400969
Permalink/DOI: https://dx.doi.org/10.14716/ijtech.v9i5.825

RFID technology operates in the LF band (125–134 kHz), the HF band (13.56 MHz), the Ultra-high frequency (UHF) band (860–960 MHz) and the microwave band (2.45 GHz and 5.8 GHz), the last of which uses the antenna's far field electromagnetic properties and enables interrogations over a long reading range (Foster & Bueberry, 1999). When operating at microwave frequencies, the RFID reader design becomes crucial, especially the RF front end circuit including the antenna element (Kumagai et al., 2011; Hattan et al., 2012).

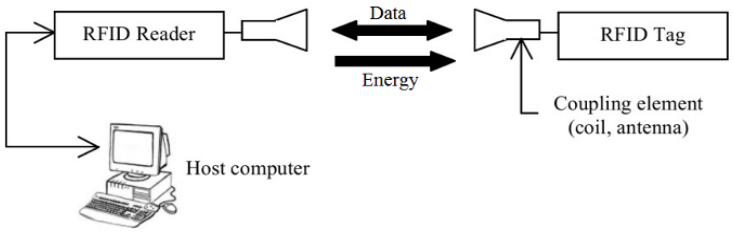

Figure 1 Block diagram of RFID system

In the literature, wireless communication devices mostly employ integrated compact microstrip patch antennas due to their light weight, low profile, low cost and easy fabrication, which allows better efficiency and wide bandwidth (Chen, 2002; Chen & Chen, 2004; Abbas et al., 2012; Roy et al., 2014; Zulkifli & Saputro, 2016). Hence they are good candidates for RFID applications. Several printed antennas have been designed for dual band RFID applications in the UHF band (860–960 MHz) and the microwave band (2.45–5.8 GHz); such configurations enable the reader to cover the different allocated frequency bands for RFID technology. A miniaturised multifrequency antenna with circular ring and Y-shaped strip was designed for WiMAX and WLAN operations (Anabi et al., 2011). The Minkowski fractal microstrip antenna presented in (Ghiotto et al., 2006) operates at 868 MHz and 2.45 GHz with radiating patch dimensions of 66×66 mm^2. In (Sabran et al., 2011), a dual frequency band antenna with an overall size of 190×190×7.635 mm^3 was achieved by controlling the shape and size of the diamond shaped patch; the obtained bandwidths were 18 MHz (902–920 MHz) and 80 MHz (2.42–2.5 GHz) in the UHF band ISM bands, respectively. This antenna includes an aluminium plate with a fixed 5 mm air gap, which makes it voluminous and complex to achieve. (Mabaso & Kumar, 2018) presents a dual band antenna consisting of a rectangular patch which is fed by the coaxial probe feeding technique; the ground plane is loaded with two rectangular strip slots and one elliptical slot with dimensions of 50×50 mm^2.

In this paper, a new design of a compact dual-band slot antenna fed by a microstrip line is proposed. Good dual-band impedance bandwidths and acceptable radiation characteristics for use in 868 MHz/2.45 GHz RFID operations can be achieved by controlling both the shapes and the dimensions of the embedded slots. The slots have been carefully designed to reduce current distribution and ensure successful performance of the antenna. With regard to regular antennas presented in previous articles, the slotted antenna excited by a microstrip line exhibits good performances in terms of compactness, simplified design, wider bandwidth, low cost, less conductor loss, and better isolation between the radiating element and the feeding network. Both simulation and optimisation of the antenna were carried out with Computer Simulation Technology Microwave Studio (CST MWS) and are discussed and described in the following sections.

2. ANTENNA DESIGN AND PERFORMANCE

The configuration of the proposed dual-band antenna is shown in Figure 2, in which a rectangular patch antenna has an inverted L shaped slot and two rectangular slots embedded in the top of the patch.

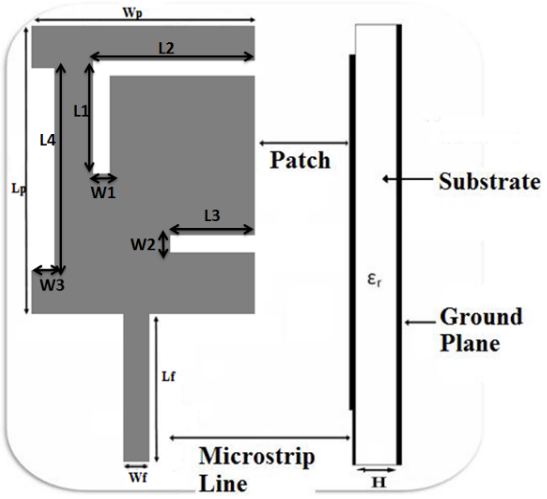

Figure 2 Geometry of the slotted antenna

The antenna was etched on an FR4_epoxy substrate of 47×46 mm^2 with a dielectric constant equal to 4.4 and thickness of the substrate H = 1.6 mm. A microstrip fed line was chosen to excite the radiating patch, which can enhance the bandwidth and gain of the proposed structure.

The design procedure of the initial geometry of the proposed antenna is derived from the standard equations discussed in (Balanis, 2005) at a resonant frequency of 2.45 GHz.

The width of the rectangular patch is calculated using the following equation:

$$w = \frac{c}{2f_r}\sqrt{\frac{2}{1+\varepsilon_r}} \tag{1}$$

The effective dielectric constant is expressed by:

$$\varepsilon_{eff} = \frac{1+\varepsilon_r}{2} + \frac{\varepsilon_r - 1}{2}\left[\frac{1}{\sqrt{1+12\frac{h}{w}}}\right] \tag{2}$$

The length extension is given by:

$$\frac{\Delta L}{h} = 0.412\frac{\left(\varepsilon_{eff}+0.3\right)\left(\frac{w}{h}+0.264\right)}{\left(\varepsilon_{eff}-0.258\right)\left(\frac{w}{h}+0.8\right)} \tag{3}$$

The effective length of the patch is given by:

$$L_{eff} = \frac{c}{2f_r\sqrt{\varepsilon_{eff}}} \tag{4}$$

The length of rectangular patch is given by:

$$L = L_{eff} - 2\Delta L \tag{5}$$

The dual-band slot antenna consists of an inverted L-shaped slot on the top and a rectangular slot on the bottom which control the two resonance frequencies. The dimension of the inverted L-shaped slot as a function of the guide wavelength (λ_g) is expressed by:

$$\lambda_g = \frac{\lambda_0}{\sqrt{\varepsilon_{eff}}} \tag{6}$$

The constant ε_{eff} denotes the effective dielectric permittivity calculated using Equation 2, and $\lambda_0 = \frac{c}{f}$ is the wavelength in free space. In this case, λ_g at frequency 2.45 GHz is 110.15 mm and λ_g at frequency 868 MHz is 210.33 mm. The total length of the inverted L slot (L_1+L_2) is 43.8 mm.

The relationship between the central resonance frequency fr of 0.868Ghz and the total length L_{T1} (L_1+L_2) can be expressed approximately by: $L_{T1}=0.2\lambda_g$. The second frequency appears by introducing a rectangular slot of length L_{T2} (L_3). The total length of the second L slot (L_3) is 11.2 mm. This length can be expressed approximately by: $L_{T2}=0.1\lambda_g$.

The final optimised dimensions of the antenna are illustrated in Table 1.

Table 1 Dimensions of the proposed antenna (unit in mm)

Parameter	Value	Parameter	Value
Lsub	47	L3	11.2
Wsub	46	L4	21
Lp	27.2	Lf	18
Wp	37	Wf	1.5
L1	14	W1 = W2	2
L2	29.8	W3	4

3. RESULTS AND DISCUSSION

3.1. Simulation Results

Optimisation of the antenna performance was conducted using Computer Simulation Technology CST simulation software, which provides different techniques and optimisation methods. A second study using Advanced Design System (ADS) software was conducted to compare the obtained results. The information presented in Figure 3 shows the resulting reflexion coefficient obtained using CST and ADS.

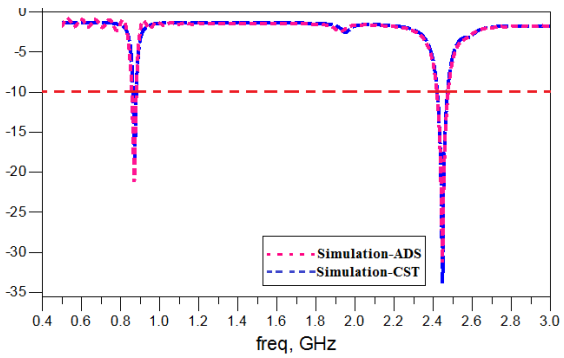

Figure 3 Comparison of simulated reflection coefficient obtained using CST and ADS

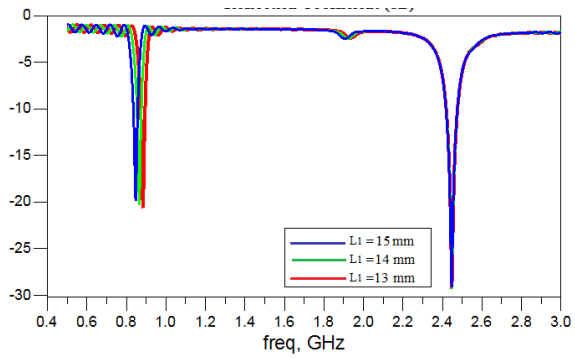

Figure 4 Simulated reflection coefficient of the proposed dual band antenna with varied L_1 while the other parameters are fixed

It is clear that close agreement was achieved between the simulation results obtained from the two types of simulation software.

The reflexion coefficient of the designed dual band antenna depends on different parameters. The simulated reflection coefficient plots with varied L_1 are shown in Figure 4. The analysis results show that the lower resonant frequency decreases as L_1 increases while the first band remains constant. Variations in the simulated reflection coefficient curves as a function of L_2 are shown in Figure 5. We observed that the lower resonant frequency decreases when L_2 increases.

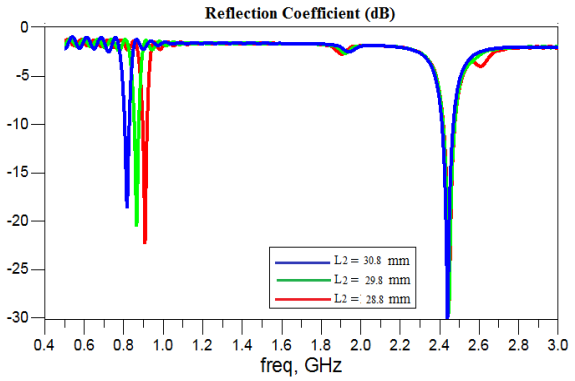

Figure 5 Simulated reflection coefficient with varied L_2 while the other parameters are fixed

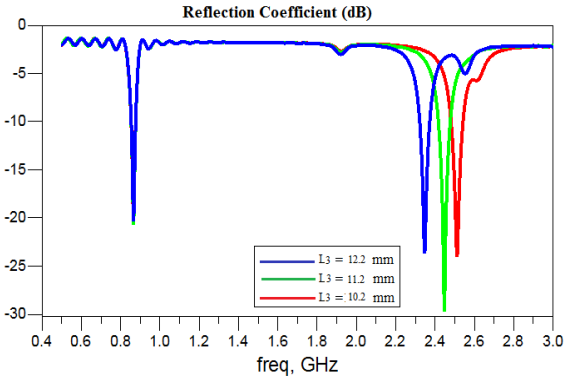

Figure 6 Simulated reflection coefficient with varied L_3 while the other parameters are fixed

The simulated reflection coefficient curves with varied L_3 are shown in Figure 6. This graph shows that the centre frequency of the second band decreases as L_3 increases. According to this analysis, the two desired working frequency bands can be tuned independently by changing the values of the lengths of the inserted slots respectively.

To obtain a better understanding the effect of the slots on the structure radiation behaviour, an investigation of the surface currents was done. The results are shown in Figure 7. It is clear that the surface current distributions at 0.868 GHz and 2.45 GHz are not similar. At the lower frequency, most of the surface current is concentrated near the inverted L slot. As indicated in Figure 7b, the surface current distribution is mainly strong on the short slot of the rectangular patch and it is also concentrated along the feed line at 2.45 GHz.

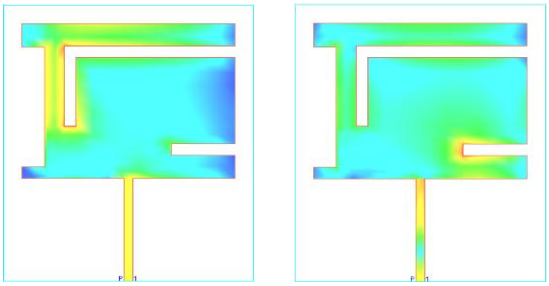

(a) (b)

Figure 7 Current distributions of the designed antenna at: (a) 0.868 GHz; and (b) 2.45 GHz

The simulated two-dimensional 2D radiation patterns in the E-plane are shown in Figure 8. The antenna is slightly directional in the low and high frequency bands because the presence of the metallic ground plane acts as a reflector.

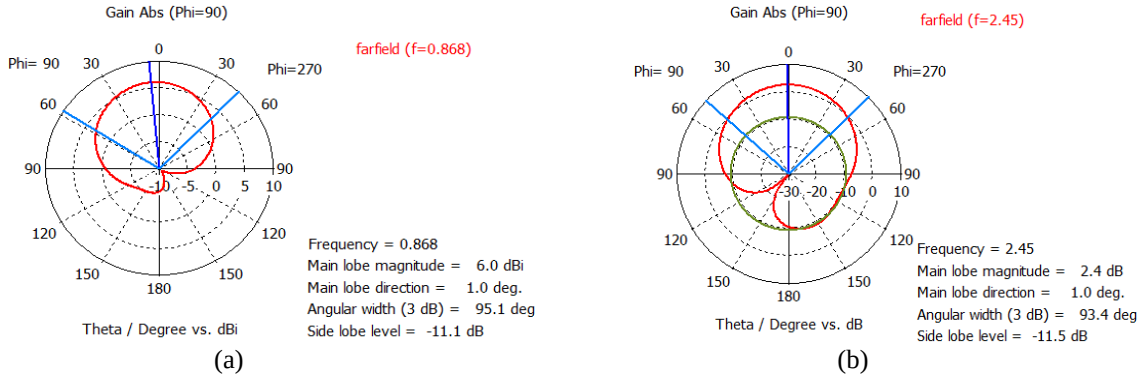

(a) (b)

Figure 8 Simulated 2D radiation patterns in the E-plane for the proposed antenna at: (a) 0.868 GHz; and (b) 2.45 GHz

The simulated 2D radiation patterns in the H-plane are shown in Figure 9. This demonstrates that the antenna is bidirectional in the high frequency of 2.45 GHz.

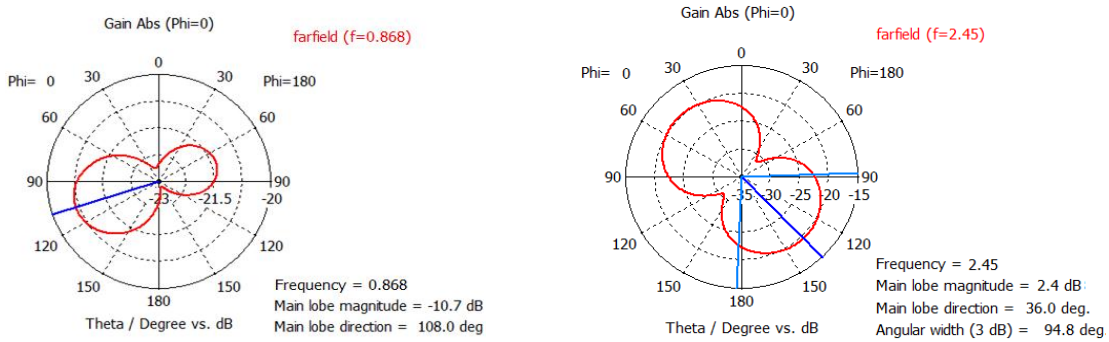

(a) (b)

Figure 9 Simulated 2D radiation patterns in the H-plane for the proposed antenna at: (a) 0.868 GHz; and (b) 2.45 GHz

3.2. Experimental Results

After validating the designed structure using a simulation, we advanced to the fabrication stage. A prototype of the antenna was fabricated using a LPKF machine and it was tested using a Vector Network Analyzer (VNA) from Agilent Technologies. The fabricated structure is shown in Figure 10.

Figure 10 Photograph of the fabricated structure

After calibrating the VNA, the electrical and radiation characteristics were determined. The simulated and measured return loss versus frequency results are shown in Figure 11.

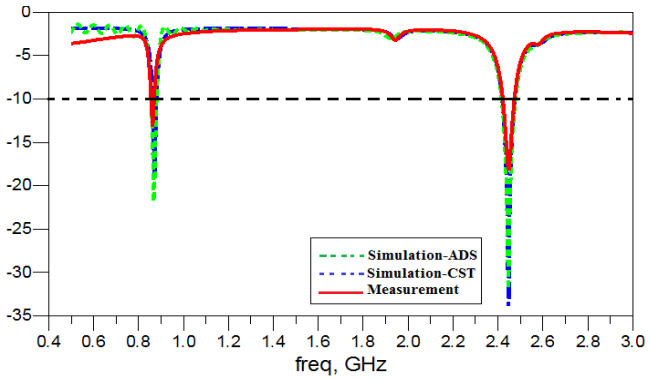

Figure 11 Simulated and measured return loss versus frequency

The deviation between the measured and simulated results is mainly due to the effect of soldering at the Sub-Miniature version A SMA connector; moreover, the slight variation of the dielectric permittivity dissipation factor at high frequencies could be caused by a limitation in the printed circuit board PCB fabrication resolution, which mainly affects the wedges of the slots. The measured reflection coefficient curve shows that the proposed antenna is fed at 2.45 GHz with a 10 dB return loss bandwidth of 90 MHz (2.41–2.5 GHz) and at 0.868 GHz with an impedance bandwidth of 28MHz (0.850–0.878 GHz).

The measurement of the radiation patterns was done in an anechoic chamber (Figure 12).

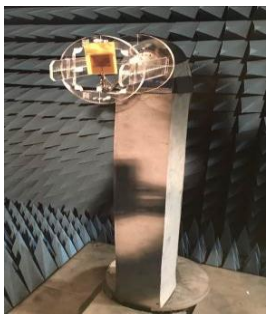

Figure 12 Proposed antenna tested in an anechoic chamber

Figures 13 and 14 present the measured radiation patterns in the E-plane and the H-plane for the two validated bands: 0.868 GHz and 2.45 GHz. The measurement results show that the realised antenna radiates nearly directionally in the E-plane and omnidirectionally in the H-plane at the two working frequency bands.

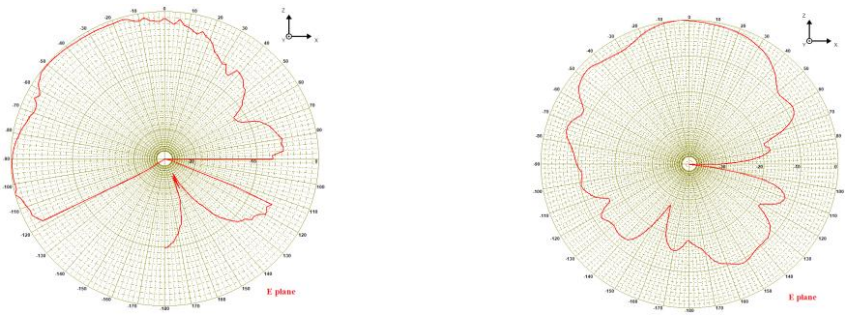

(a) (b)

Figure 13 Measured radiation patterns at: (a) 0.868 GHz; and (b) 2.45 GHz, in the E-plane

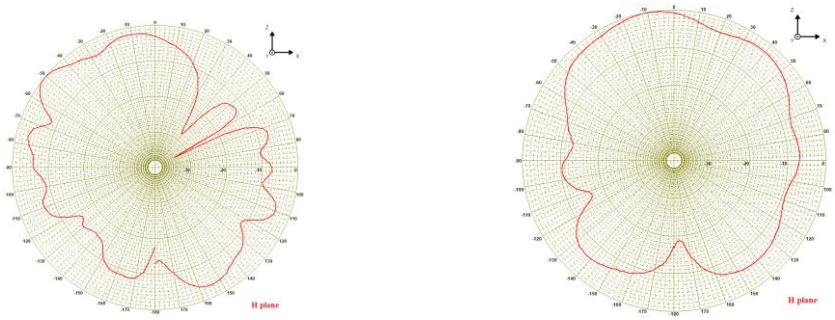

(a) (b)

Figure 14 Measured radiation patterns at: (a) 0.868 GHz; and (b) 2.45 GHz, in the H-plane

To highlight the contribution of this work in terms of antenna performances with regard to size, resonance frequency and gain, we conducted a comparative study of our proposed antenna with similar state-of-the-art antennas presented in the current literature. The results are detailed in Table 2. It worth noting that the comparison demonstrates that the proposed work exhibits good features appropriate for dual-band RFID applications at UHF bands.

Table 2 The performance of the designed antenna in comparison to other antennas in the literature

Published literature versus proposed work	Antenna size (mm^2)	Resonance frequency (GHz)	Return loss (dB)		BW (MHz)	
			F_1	F_2	F_1	F_2
Ihamji et al. (2017)	71×94	0.915/2.45/5.8	-11	-10	52	80
Ennajih et al. (2018)	75×50	0.900/2.45	-13	-23	87	516
El Hamraoui et al. (2018)	48×47	0.915/2.45	-14.5	-26.7	28	100
Gmih et al. (2018)	60×74	0.92	-25.41	-	54	-
Proposed work	47×46	0.868/2.45	-12	-18	28	90

4. CONCLUSION

A new dual-band and miniature microstrip antenna was numerically and experimentally studied. By optimising the lengths and the locations of the inserted slots, it is possible to obtain the two resonating frequencies for the desired bands for RFID applications. The simulated and experimental results validate the proposed antenna with two bandwidths: 90 MHz (2.41–2.5 GHz) and 28 MHz (0.850–0.878 GHz). According to these results, the dual-band antenna can cover the RFID UHF in the European region and microwave bands (2.45 GHz bands). Hence, the proposed antenna is an excellent candidate for handheld RFID readers.

5. ACKNOWLEDGEMENT

The authors would like to thank Mr Mohamed Latrach, Professor in ESEO, Engineering Institute in Angers, France for providing support and assistance to perform the simulations using software and to obtain the measurements using the VNA and the anechoic chamber available in his laboratory.

6. REFERENCES

Abbas, S.M., Aftab, B., Qamar, E., Muzahir, F., Shahid, S., Zahra, H., 2012. High Gain Broadband Monopole Antenna for Wireless Communications. *IEEE Antennas And Propagation Letters*, Volume 156, pp. 766–770

Anabi, K.H., Mandeep, J.S., Islam, M., Tiang, J.J., 2011. A Quarter-wave Y-shaped Patch Antenna with Two Unequal Arms for Wideband Ultra High Frequency Radio-frequency Identification (UHF RFID) Operations. *International Journal of the Physical Sciences*, Volume 6(26), pp. 6200–6209

Balanis, C.A., 2005. *Antenna Theory Analysis and Design*. 3rd Edition. USA: John Wiley & Sons, Inc

Brown, D., 2007. *RFID Implementation.* New York: McGraw-Hill Inc

Chen, H.M., 2002. Microstrip-fed Dual-frequency Printed Triangular Monopole. *Electronic Letters*, Volume 38, pp. 619–620

Chen, H.D., Chen, H.T., 2004. A CPW-fed Dual-frequency Monopole Antenna. *IEEE Transactions on Antennas and Propagation*, Volume 52(4), pp. 320–326

El Hamraoui, A., El Abdelmounim, Zbitou, J., Bennis, J., Latrach, M., 2016. Compact Dual-band Microstrip Slot Antenna for UHF and Microwave RFID Applications. *In:* Oral Presentations in the 11th IEEE International Conference on Intelligent Systems: Theories and Applications (SITA) Conference, Mohammadia, Morocco

El Hamraoui, A., El Abdelmounim, Zbitou, J., Errkik, A., Bennis, H., Latrach, M., 2018. A Dual-band Microstrip Slotted Antenna for UHF and Microwave RFID Readers. *Telecommunication, Computing, Electronics and Control* (*TELKOMNIKA),* Volume 16(1), pp. 94–101

Ennajih, A., Zbitou, J., Latrach, M., Errkik, A., 2018. A Novel Design of a Miniature Metamaterial Antenna for RFID Reader Applications. *Telecommunication, Computing, Electronics and Control (TELKOMNIKA),* Volume 16(1), pp. 174–181

Finkenzeller, K., 2010. *RFID Handbook: Fundamentals and Applications in Contactless Smart Cards and Identification*. 3rd Edition. New York: John Wiley and Sons Inc

Foster, P., Bueberry, R., 1999. Antenna Problems in RFID systems. *In:* IEE Colloquium on RFID Technology, 25 October 1999, London, pp. 3/1–3/5

Ghiotto, A., Ibrahiem, A., Vuong, T.P., Tedjini, S., 2006. New Bi-band Fractal Antennas. *In:* Oral Presentations in 12th IEEE International Symposium on Antenna Technology and Applied Electromagnetics [ANTEM] and the Canadian Radio Sciences (CNC-URSI) [URSI] Conference, July, Montréal, Canada

Gmih, Y., El Hachimi, Y., Makroum, M., Farchi, A., 2018. A Miniature RFID Antenna at UHF Band using Meander-line Technique. *International Journal of Electrical and Computer Engineering (IJECE).* Volume 8(4), pp. 2280–2289

Hattan, F., Abutarboush, H., Nilavalan, R., Cheung, S.W., 2012. Multiband and Wideband Monopole Antenna for GSM900 and Other Wireless Applications. *IEEE Antennas and Wireless Propagation Letters*, Volume 11, pp. 716–720

Ihamji, M., El Abdelmounim, Bennis, H., Hefnawi, M., Latrach, M., 2017. Design of Compact Tri-band Fractal Antenna for RFID Readers. *International Journal of Electrical and Computer Engineering (IJECE),* Volume 7(4), pp. 2036–2044

Kumagai, T., Saito, K., Takahashi, M., 2011. A Small 915 MHz Receiving Antenna for Wireless Power Transmission Aimed at Medical Applications. *International Journal of Technology*, Volume 2(1), pp. 20–27

Mabaso, M., Kumar, P., 2018. A Dual Band Patch Antenna for Bluetooth and Wireless Local Area Networks Applications. *International Journal of Microwave and Optical Technology.* Volume 13(5), pp. 393–400

Mujahid, U., Najam-ul-islam, M., 2015. Pitfalls in Ultralightweight RFID Authentication Protocol. *International Journal of Communication Networks and Information Security (IJCNIS)*, Volume 7(3), pp. 169–176

Paret, A., 2008. *RFID en Ultra et Super Hautes Fréquences UHF-SHF, Théorie et Mise en Œuvre.* Dunod

Poespawati, N.R., Nugroho, M.R., 2016. Design and Fabrication of a Solar Power System for an Active RFID Tag. *International Journal of Technology*, Volume 7(4), pp. 720–728

Roy, A., Choudhary, P.K., Anand, S., Sarkar, P.P., Bhunia, S., 2014. A Novel Approach on Miniaturization of Microstrip Patch Antenna with Loaded Strips. *In:* Electronics, Communication and Instrumentation (ICECI), International Conference, 16-17 January, Kolkata, India, pp. 1–4

Sabran, M.I., Rahim, S., Rahman, A., 2011. A Dual-band Diamond-shaped Antenna for RFID Application. *IEEE Transactions on Antennas and Propagation Letters*, Volume 10, pp. 979–982

Zulkifli, F.Y., Saputro, N.A., 2016. Left-handed Metamaterial (LHM) Structure Stacked on a Two-element Microstrip Antenna Array. *International Journal of Technology*, Volume 7(4), pp. 683–690